

# Lattice Boltzmann simulations of three-dimensional single droplet deformation and breakup under simple shear flow

Haowen Xi\* and Comer Duncan†

*Department of Physics and Astronomy, Bowling Green State University, Bowling Green, Ohio 43403*

(Received 24 July 1998)

We present three-dimensional numerical simulations of the classical Taylor experiment on droplet deformation within a shear flow. We have used the promising lattice Boltzmann method numerical scheme to simulate single droplet deformation and breakup under simple shear flow. We first compute the deformation of the droplet, and find excellent agreement with the theoretical prediction. We have used the same method to simulate the shear and breakup for larger values of the shear rate. We find that the lattice Boltzmann method used in conjunction with the interface force model of Shan and Chen [Phys. Rev. E **47**, 1815 (1993); **49**, 2941 (1994)] results in an excellent treatment of the entire process from small deformation to breakup into multiple droplets. Our results could be extended to study the rheology of dispersed droplets and the dynamics of droplet breakup and coalescence in shear flow. [S1063-651X(99)13603-1]

PACS number(s): 47.55.Dz, 47.55.Kf, 05.50.+q

## I. INTRODUCTION

The effect of shear flow on droplets of one fluid freely suspended in another immiscible fluid is a problem of long-standing interest [1–5]. Long ago Taylor [6,7] considered a droplet of a Newtonian fluid suspended in the shear flow of a second Newtonian fluid. He estimated the largest stable droplet radius by balancing the surface stresses due to interfacial tension and viscous stress due to shear. Taylor found that the deformation of the droplet can be expressed in terms of three dimensionless parameters: the capillary (or Taylor) number  $Ca = R \eta_m \dot{\gamma} / \beta$ , the viscosity ratio  $\lambda = \eta_d / \eta_m$ , and the density ratio  $\kappa = \rho_d / \rho_m$ . Here  $\beta$  is the interfacial tension coefficient,  $\dot{\gamma}$  is the shear rate, and  $R$  is the droplet radius.  $\eta_d$  and  $\eta_m$  are the droplet and medium viscosity, respectively, and  $\rho_d$  and  $\rho_m$  are the droplet and medium density, respectively. For two fluids of equal viscosity ( $\lambda = 1$ ) and equal density (neutrally buoyant,  $\kappa = 1$ ) under simple shear flow, Taylor obtained a theoretical result for *small* deformation  $D$ , where

$$D = (L - B) / (L + B) = \frac{19\eta_d + 16\eta_m}{16\eta_d + 16\eta_m} = (35/32)Ca. \quad (1)$$

Here  $L$  and  $B$  are the largest and smallest distances from the droplet surface from its center (the ‘‘major’’ and ‘‘minor’’ axes). Thus, for a spherical droplet,  $D$  is equal to zero.

From the numerical simulation point of view, the simulation of droplet deformation and breakup problem is very difficult. The conventional numerical modeling of a liquid-liquid system, which involves solving hydrodynamic partial differential equations, has seen only limited success [5]. The equations of motion of flow field must be solved both inside and outside the droplet, with the appropriate boundary condition applied on the interface between the interior and exte-

rior of the droplet. However, the shape of the droplet is not known *a priori*, and must be determined as part of the solution. Because of these complications, there have not been many successful three-dimensional numerical studies of droplet deformation and breakup. The case of many drops under shear flow where *both* breakup and coalescence (resulting from the collisions of droplets) effects are taken into account is largely unexplored [5]. In this paper, we report the use of an alternative and promising numerical scheme called the lattice Boltzmann method (LBM) [8–11] to simulate the deformation of droplets under shear. In recent years there have been a growing number of successful applications of LBM to a variety of physical systems. The basic idea of the LBM is to construct simplified kinetic models that incorporate the essential physics of microscopic dynamics, so that the macroscopic averaged properties obey the desired macroscopic Navier-Stokes equations. One of the great advantages of the LBM is that the information about the phase boundary (e.g., interface boundary between droplets and the exterior medium), the droplet size and shape, and the flow field can all automatically arise from the solutions. The LBM scheme has been shown to be particularly successful in multiphase flow dynamics [12–14] and flow in systems with complex boundaries [8,11]. However, there have been only few quantitative studies reported of three-dimensional multiphase flow problems using the LBM. In this paper, we will present a three-dimensional numerical study of droplet deformation using the LBM with quantitative comparison with theoretical results in the small deformation regime. An early study [15] of droplet deformation was restricted to two-dimensional space with no quantitative comparison between the numerical simulations and the theoretical results for droplet deformation. The comparison between the simulations of three-dimensional droplet shear with the theoretical results of Taylor represents an important step in the validation of the applicability of the LBM method to such physical systems.

The mechanical dispersion of immiscible droplets is of importance both in nature and in many industrial applications [1–3]. The mixing process under shear flow is usually

\*Electronic address: haowen@bgnet.bgsu.edu

†Electronic address: gcd@chandra.bgsu.edu

divided into three stages: (i) stretching and deformation of liquid droplets, (ii) breakup of these droplets, and (iii) coalescence of the resulting droplets upon collision. The basic process of deformation of a liquid droplet, immersed in the given flow field of a second (immiscible) liquid is governed by the capillary number, which is the ratio of the deforming shear stress applied externally and the shape-conserving interfacial tension. One good example of the dispersion of droplets is the blending of molten polymer systems [16]. Because nearly all chemically different polymers are immiscible, the effective mixing of immiscible polymers is a ubiquitous industrial goal. The usual objective is to produce a fine dispersion of submicron-sized particles of one polymer in a matrix of another polymer, with the goal of producing a composite system with improved physical properties. Thus the rheology of the dispersion of droplets in various shear flows at low Reynolds numbers is of both practical and fundamental interest, and has received considerable attention over the past 60 years, starting with early work by Taylor in 1934. For recent references, see Refs. [4,5].

This paper is organized as follows: In Sec. II we present a brief discussion of the multicomponent LBM and outline our numerical techniques. In Sec. III, we present quantitative numerical results for two studies. First, we make a comparison between the simulation of small deformation droplet with the classical Taylor theory. Second, we report on simulations with a larger shear rate in which the initial droplet is deformed, then sheared to breakup. We conclude with a discussion of some of the interesting problems which are opened up given the utility of the three-dimensional LBM to systems of droplets under various shear flow conditions.

## II. NUMERICAL MODEL

In this section, we present a brief description of the LBM for modeling multicomponent immiscible fluids developed by Shan and Chen (SC) [17,18]. Denote by  $n_a^\sigma(\mathbf{x}, t)$  the number density of  $\sigma$ th particles at spatial point  $\mathbf{x}$  and time  $t$  for the fluid ( $\sigma=1$  and 2) with velocity  $\mathbf{e}_a$ . Here  $a=0, \dots, b$ , where  $b$  is the number of velocity directions on a three-dimensional lattice (in the D3Q19 lattice model,  $b=18$ ) [19]. The LBM for the particle distribution function  $n_a^\sigma(\mathbf{x}, t)$  can be written as

$$n_a^\sigma(\mathbf{x} + \mathbf{e}_a, t+1) - n_a^\sigma(\mathbf{x}, t) = -\frac{1}{\tau^\sigma} [n_a^\sigma(\mathbf{x}, t) - n_a^{\sigma(eq)}(\mathbf{x}, t)], \quad (2)$$

where  $n_a^{\sigma(eq)}(\mathbf{x}, t)$  is the local equilibrium distribution function which depends on the microscopic velocity  $\mathbf{e}_a$ , the macroscopic density  $n_a$ , and the velocity  $\mathbf{u}$ , and  $\tau^\sigma$  is the relaxation time for species  $\sigma$  and controls the rate of approach to equilibrium for that species. The Galilean-invariant three-dimensional D3Q19 lattice model equilibrium distribution function can be represented as

$$n_a^{\sigma(eq)}(\mathbf{x}, t) = \frac{1}{3} n^\sigma(\mathbf{x}, t) [1 - \frac{3}{2} \mathbf{u} \cdot \mathbf{u}], |\mathbf{e}_a|^2 = 0, \quad (3)$$

$$n_a^{\sigma(eq)}(\mathbf{x}, t) = \frac{1}{18} n^\sigma(\mathbf{x}, t) [1 + 3(\mathbf{e}_a \cdot \mathbf{u}) + \frac{9}{2}(\mathbf{e}_a \cdot \mathbf{u})^2 - \frac{3}{2} \mathbf{u} \cdot \mathbf{u}], \quad (4)$$

$$|\mathbf{e}_a|^2 = 1,$$

$$n_a^{\sigma(eq)}(\mathbf{x}, t) = \frac{1}{36} n^\sigma(\mathbf{x}, t) [1 + 3(\mathbf{e}_a \cdot \mathbf{u}) + \frac{9}{2}(\mathbf{e}_a \cdot \mathbf{u})^2 - \frac{3}{2} \mathbf{u} \cdot \mathbf{u}], \quad (5)$$

$$|\mathbf{e}_a|^2 = 2,$$

where the macroscopic density  $n^\sigma(\mathbf{x}, t)$  and velocity for each fluid component  $\sigma$  are defined as

$$n^\sigma(\mathbf{x}, t) = \sum_a n_a^\sigma(\mathbf{x}, t) \quad (6)$$

and

$$\mathbf{u}(\mathbf{x}, t) = \frac{\sum_\sigma m^\sigma \sum_a n_a^\sigma \mathbf{e}_a / \tau^\sigma}{\sum_\sigma m^\sigma \sum_a n_a^\sigma / \tau^\sigma} + \frac{\tau^\sigma}{\sum_a m^\sigma n_a^\sigma(\mathbf{x}, t)} \frac{d\mathbf{p}^\sigma}{dt}, \quad (7)$$

where  $m^\sigma$  is the mass of the  $\sigma$ th component. Note that for the  $\sigma$ th component the macroscopic mass density and momentum density are defined to be  $\rho_\sigma = m^\sigma n^\sigma$  and  $\rho_\sigma \mathbf{u}_\sigma = m^\sigma \sum_a n_a^\sigma \mathbf{e}_a$ , respectively. The second term in Eq. (7) represents the interaction between the two fluid components. In order to model surface tension forces, SC introduced an interaction potential  $V(\mathbf{x}, \mathbf{x}') = -G^{\sigma\sigma'}(\mathbf{x}, \mathbf{x}') \psi^{\sigma'}(\mathbf{x}') \psi^\sigma(\mathbf{x})$ . Here  $\psi^\sigma(\mathbf{x}) = F[n^\sigma(\mathbf{x})]$  is a function of density  $n^\sigma(\mathbf{x})$ , and  $G^{\sigma\sigma'}(\mathbf{x}, \mathbf{x}')$  is the interaction strength. Assuming only nearest-neighbor interactions for simplicity, and using  $\psi^\sigma(\mathbf{x}) = n^\sigma(\mathbf{x})$  with  $G_a^{\sigma\sigma} = 0$  and  $G_a^{\sigma\sigma'} \neq 0$  for  $\sigma \neq \sigma'$ , one obtains

$$\frac{d\mathbf{p}^\sigma}{dt} = -n^\sigma(\mathbf{x}) \sum_{\sigma'} \sum_a G_a^{\sigma\sigma'} n^{\sigma'}(\mathbf{x} + \mathbf{e}_a) \mathbf{e}_a. \quad (8)$$

In a practical numerical study, one often assumes that  $G_a^{\sigma\sigma'}$  is given by a constant  $G$ , and then varies the value of  $G$  to model the surface tension strength. However, one must be careful about the treatment of  $G_a^{\sigma\sigma'}$ , and should use the values that insure the Galilean invariance of the macroscopic equation in three-dimensional space. For the three-dimensional D3Q19 lattice model we use in the present study, after the correct projection from the four-dimensional FCHC lattice [20], one obtains

$$G_a^{\sigma\sigma'} = G, \quad |\mathbf{e}_a|^2 = 1,$$

$$G_a^{\sigma\sigma'} = G/2, \quad |\mathbf{e}_a|^2 = 2,$$

$$G_a^{\sigma\sigma'} = 0 \quad \text{otherwise.} \quad (9)$$

## III. NUMERICAL SIMULATIONS AND DISCUSSION

### A. Small deformation limit of droplet shear

We now present our numerical study of the classical Taylor experiment, i.e., the deformation of a single droplet under simple shear flow. The shear velocity is given by

$$\mathbf{v} = (\dot{\gamma}z, 0, 0) = (2Uz/L_z, 0, 0), \quad (10)$$

where  $-L_z/2 \leq z \leq +L_z/2$ , and  $L_z$  is the distance between the top boundary plane which moves with velocity  $+U$  and bottom boundary plane which moves with velocity  $-U$ . Taylor obtained the theoretical prediction given in Eq. (1) for the dimensionless *small* deformation  $D$ . With  $\lambda=1$  and  $\kappa=1$ , where  $Ca$  defined as above, we have

$$Ca = \frac{\dot{\gamma} R \nu \rho}{\beta} = \frac{U}{L_z/2} \frac{R \nu \rho}{\beta}. \quad (11)$$

Here  $\nu$  and  $\rho$  are the kinematic viscosity and the density of the fluid, respectively. In our numerical simulation, we have chosen the densities  $\rho = \rho_1 = \rho_2 = 0.3$  with  $m^1 = m^2 = 1$ , and viscosities  $\nu = \nu_1 = \nu_2 = (2\tau - 1)/6$  with  $\tau = \tau_1 = \tau_2 = 1.0$ . The initial radius  $R$  of the drop was set to 10.0. The system size was chosen to be  $L_x \times L_y \times L_z = 128 \times 62 \times 62$ . We used parameter values  $G_{12} = G_{21} = 0.5$  and  $G_{11} = G_{22} = 0.0$  for modeling the surface tension. The actual value of surface tension  $\beta$  was determined by placing a single droplet in the medium in the absence of shear flow, and using the Laplace law  $\delta p = 2\beta/R$ , where  $\delta p$  is the pressure difference inside and outside the droplet and  $R$  is the radius of the droplet. Once we have all the numerical values  $(R, \nu, \rho, \beta, L_z)$ , the only free parameter left is the shear velocity  $U$ , which we can vary to determine the Taylor number  $Ca$ . The initial condition for the simulation was taken to be a single droplet placed in the center of the computational volume with equal constant density both inside and outside the droplet. The initial macroscopic velocity field  $\mathbf{u}$  was set to zero everywhere. In order to determine the ‘‘major’’ and ‘‘minor’’ axes  $L$  and  $B$ , numerically we follow the standard technique used in classical mechanics for calculating the rotational inertia  $I_{ij}$ . We first calculate the symmetric matrix  $A_{ij}$  defined as

$$A_{ij} = \frac{\int \int \int \rho x_i x_j dx dy dz}{\int \int \int \rho dx dy dz}, \quad (12)$$

where the origin of the coordinates is located at the center of the initial droplet, and  $x_i, i=1,2,3$  are the Cartesian coordinates at a point in the computational volume. After determining the eigenvalues of the matrix  $A_{ij}$ , we can then determine the values for  $L$  and  $B$ . We made a series of runs of the three dimensional LBM code for several small deformation-generating shear flows. For each such run we computed the values of  $L$  and  $B$  as indicated above. Figure 1 shows the comparison between our numerical results and the theoretical prediction for  $D$  vs  $Ca$ . From the figure one can see that the agreement between our numerical simulations with the LBM and the theoretical result is excellent at small Taylor number. This agreement between our LBM-computed values and the theoretical value for small deformation is clear evidence that the numerical methods perform well for small Taylor number. This validates the accuracy of the LBM plus SC model in this environment.

### B. Larger deformation to breakup

Given the successful comparison with the Taylor result in the small deformation limit, we have confidence that the

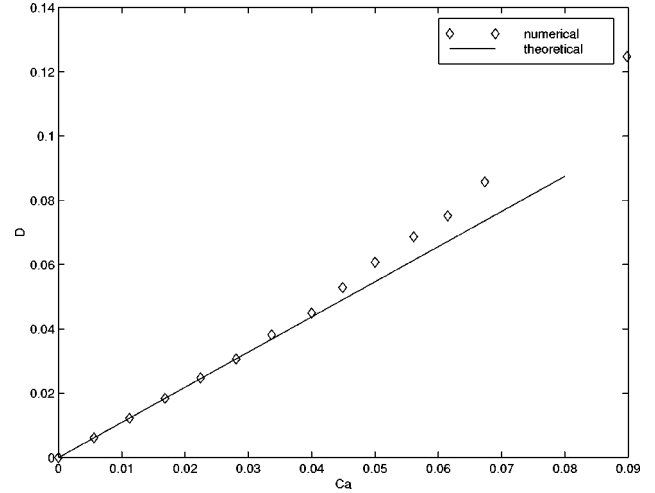


FIG. 1. Plot of deformation vs Taylor number in the small deformation limit. Also shown is the theoretical result of Taylor.

LBM plus the SC interface force model does a credible job. We have performed several simulations at larger shear rates to investigate the ability of the SC model to adequately track the deforming interface to and beyond breakup. Here we report the results of using the three-dimensional LBM code for the breakup. Our computational volume was  $128 \times 52 \times 31$ . The value of the shear velocity for this was  $U=0.5$ . The smaller value for  $L_z$  results in an effectively larger shear rate for the same value of  $U$ . This change results in a qualitatively different range of the droplet deformation and breakup. We emphasize that the same values of  $G_{12}$ ,  $G_{21}$ ,  $G_{11}$ , and  $G_{22}$  used in the small deformation limit were used for the breakup simulations. The combination of LBM and the SC model for the interface force between the two components proved to be a robust combination once the initial work was done to determine the best range for the  $G_{12}$ ,  $G_{21}$ ,  $G_{11}$ , and  $G_{22}$  parameters.

Figures 2–6 show snapshots of the evolution of the droplet under shear. The initial spherical droplet was given a radius of 8.0. The progression from deformation to breakup is illustrated in the figures via the rendering of the isosurface of the droplet in the surrounding volume of the other fluid. The figures show just the fluid corresponding to the initial

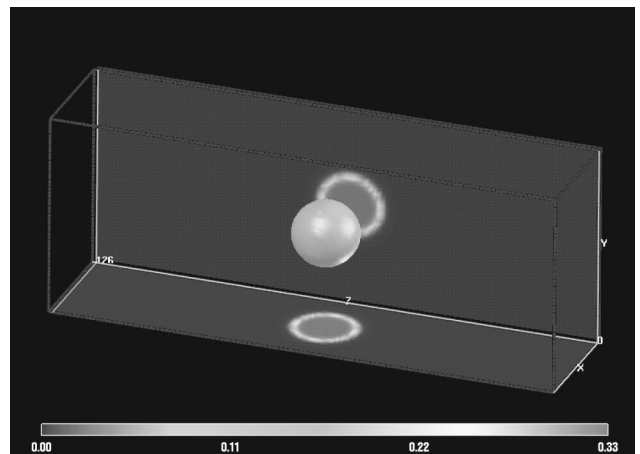


FIG. 2. Initial droplet of radius 8.0. The legend shows a grey scale color map of the density of the sheared droplet.

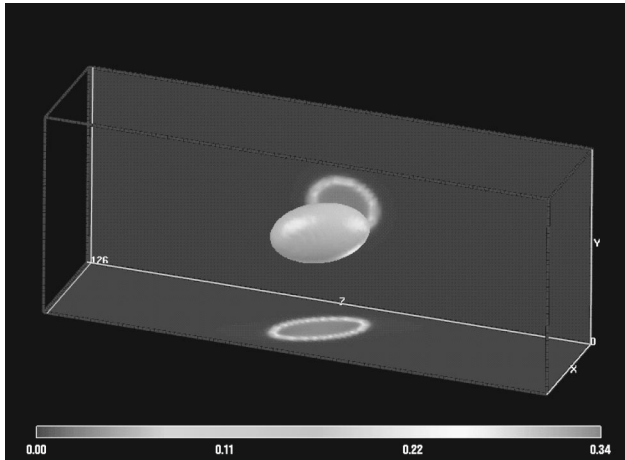


FIG. 3. Deformed droplet at 400 cycles.

droplet. A slice was taken in a vertical plane through the center of the initial droplet and the results rendered on a plane which is shown at the back side of the volume. Similarly, a second slice was taken along the long axis and parallel to the bottom of the computational volume, and projected onto the bottom of the volume's bounding box. These data show that there is considerable stretching and then pinching breakup at the ends of the long, deformed, droplet. Subsequent to the breakup the shear induces further stretching of the newly formed droplets. These in turn are eventually significantly sheared to breakup themselves. Figure 6 shows the droplets wrapping around at the long ends of the volume due to our use of periodic boundary conditions at the ends in the  $x$  direction. The generalization of these simulations to treat multiple droplet shear, breakup, and coalescence is the next step in the simulation of these systems, and is under current investigation.

#### IV. CONCLUSIONS

In the present paper we have used the LBM along with the interface model developed by Shan and Chen [17] for multiphase fluids to study single droplet deformation under simple shear flow. We have considered a three-dimensional two-fluid system with equal kinematic viscosities and densities. We calculated the deformation  $D$ , and found that the

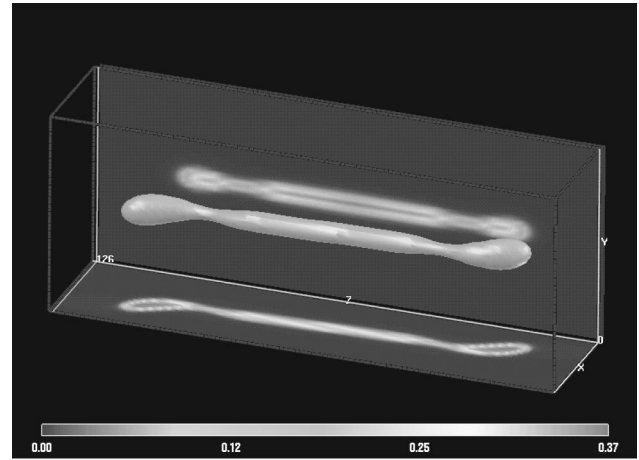


FIG. 5. Droplet at 1200 cycles just before pinched breakup at its ends.

numerical results are in excellent agreement with Taylor's theoretical results. The use of equal densities and kinematic viscosities was simply an arbitrary numerical choice. It is interesting to note that the whole range of the ratio  $\eta_d/\eta_m$  from 0 to  $\infty$  results in  $(19\eta_d + 16\eta_m)/(16\eta_d + 16\eta_m)$  varying only from 1.0 to 1.1875. Thus the small deformation  $D = (L - B)/(L + B)$  is almost equal to  $Ca$ . The fact that Taylor's prediction has been verified in this special numerical simulation indicates that the viscous stress field on the droplet surface has been correctly reproduced. It is also interesting to consider the drag force on a slowly moving droplet in a fluid. It is well known that the drag force on a slowly moving solid sphere is well described by the Stokes law formula. For a fluid droplet the picture is qualitatively different. Instead of a rigid boundary condition on the surface of the droplet, the fluid has a stress-free boundary condition. The shape of the droplet may deform, and set up recirculating flow inside the droplet. In order to calculate the drag force on the moving droplet, one needs to know the viscous stress field, as did Taylor for viscous stress due to shear. We have also simulated the effect of larger shear rates, and have successfully evolved the sheared single droplet to breakup and beyond. Thus this LBM scheme is not limited to small deformations, and is of utility for the study of the dynamics

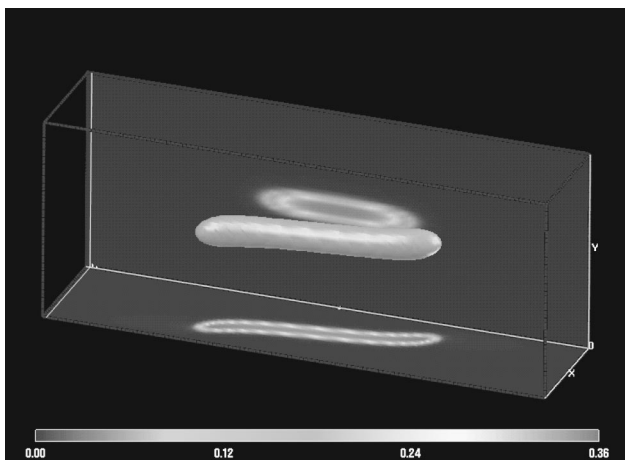


FIG. 4. Sheared droplet at 800 cycles.

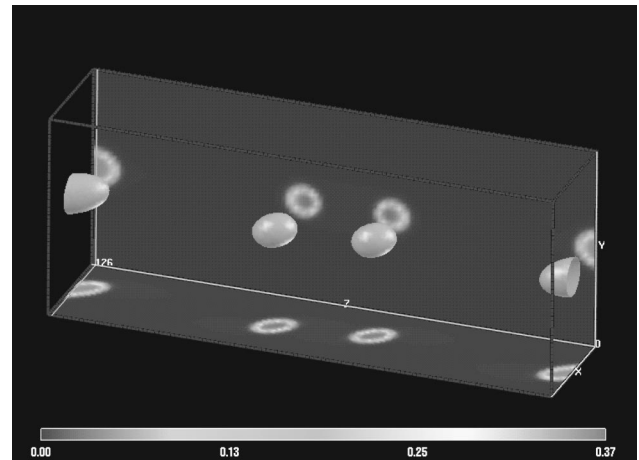


FIG. 6. Multiple droplets at 1600 cycles.

deformation and breakup of many-droplet systems. In fact, the work for computing  $N$  droplets scales linearly with  $N$ , in contrast to the conventional computational fluid dynamics for which the computational work scales  $N^2$ . Thus the LBM approach could provide the capability to study the rheology of dispersed droplets and the dynamics of many-droplet systems. Our results indicate that the LBM scheme is fully capable of predicting the merger as well as breakup [21] of many droplets systems. Such studies are currently under way. The results reported in this paper demonstrate that the LBM scheme which we have utilized could be a useful tool for a wide range of industrial problems, including polymer molding processes and the rheology of many-droplet systems.

One aspect of the present method which needs further study centers around the slightly nonrobust character of the interface model. That is, given a choice of the density ratio of the two fluids we have found the choices of the  $G_{12}$ ,  $G_{21}$ ,  $G_{11}$ , and  $G_{22}$  parameters, characterizing the strength of the interfacial forces which give a stable evolution, to reside in a somewhat narrow range. Inside the range the evolution is stable, and produces a qualitatively correct tracking of the breakup process. Outside the range, the simulations eventually fail by producing negative  $f_i$  for one or both fluids, thus inducing the halting of the computations. It would be useful to get a handle on how to extend the range

of robustness of the simulations, so that a wide range of both the density ratio and the  $G$  values can be used to increase the dynamic range of systems to which the methods can be applied. We are currently exploring the extent to which the finite difference method can be used, with the extra freedom one gains by unlocking the velocity space from the position space lattice and requiring that the Courant limit be satisfied. When used in conjunction with the SC interface model, this method will be more stable and perhaps allow a wider range of density ratios and  $G$  values. We expect to report on our investigations into these matters in a future publication.

#### ACKNOWLEDGMENTS

We thank Hudong Chen, Xiaowen Shan, Shiyi Chen, Nicos S. Martys, Xiaoyi He, and Li-Shi Luo for helpful and enjoyable discussions. This work was supported in part by NSF Grant No. ASC-9418357 for the Pharaoh MetaCenter Regional Alliance, and by the PRF under Contract No. 33160-GB9 and the Research Corporation under Grant No. CC4250. The simulations were performed on the SGI PowerChallenge at the Ohio Supercomputer Center. We thank Ken Flurchick of the Ohio Supercomputer Center for his expert assistance with the visualization of the droplet shear and breakup.

- 
- [1] H. P. Grace, Chem. Eng. Commun. **14**, 227 (1982).
  - [2] A. Acrivos, Fourth International Conference on Physiochemical Hydrodynamics [Ann. (N.Y.) Acad. Sci. **404**, 1 (1983)].
  - [3] J. M. Rallison, Annu. Rev. Fluid Mech. **16**, 45 (1984).
  - [4] M. Tjahjadi and J. M. Ottino, J. Fluid Mech. **243**, 297 (1991).
  - [5] H. A. Stone, Annu. Rev. Fluid Mech. **26**, 65 (1994).
  - [6] G. I. Taylor, Proc. R. Soc. London, Ser. A **138**, 41 (1932).
  - [7] G. I. Taylor, Proc. R. Soc. London, Ser. A **146**, 501 (1934).
  - [8] R. Benzi, S. Succi, and M. Vergassola, Phys. Rep. **222**, 145 (1992).
  - [9] “*Lattice Gas Methods for Partial Differential Equations*,” edited by G. D. Doolen (Addison Wesley, Redwood City, CA, 1989).
  - [10] D. H. Rothman and S. Zaleski, Rev. Mod. Phys. **66**, 1417 (1994).
  - [11] Shiyi Chen and Gary D. Doolen, Ann. Rev. Fluid Mech. **30**, 329 (1998).
  - [12] A. K. Gunstensen, D. H. Rothman, S. Zaleski, and G. Zanetti, Phys. Rev. A **43**, 4320 (1991).
  - [13] D. Grunau, S. Chen, and Kenneth Eggert, Phys. Rev. A **43**, 4320 (1991).
  - [14] X. Shan and G. Doolen, J. Stat. Phys. **81**, 379 (1995).
  - [15] I. Halliday and C. M. Care, Phys. Rev. E **54**, 2573 (1996).
  - [16] Scott T. Milner and Haowe Xi, J. Rheol. **40**, 663 (1996).
  - [17] X. Shan and H. Chen, Phys. Rev. E **47**, 1815 (1993).
  - [18] X. Shan and H. Chen, Phys. Rev. E **49**, 2941 (1994).
  - [19] Y. H. Qian, D. d’Humières, and P. Lallemand, Europhys. Lett. **17**, 479 (1992).
  - [20] Nicos S. Martys and Hudong Chen, Phys. Rev. E **53**, 743 (1996).
  - [21] Haowen Xi and Comer Duncan (unpublished).